ISSN 1070-3632, Russian Journal of General Chemistry, 2012, Vol. 82, No. 2, pp. 230–235. © Pleiades Publishing, Ltd., 2012.
Original Russian Text © I.I. Didenkulova, E.I. Tsyganova, V.M. Shekunova, Yu.A. Aleksandrov, 2012, published in Zhurnal Obshchei Khimii, 2012, Vol. 82, No. 2, pp. 234–239.

Mechanism of CO Oxidation on Catalysts Prepared by Pyrolysis of Transition Metal β-Diketonates on a Synthetic Ceramic Foam Matrix

I. I. Didenkulova[a], E. I. Tsyganova[a], V. M. Shekunova[a], and Yu. A. Aleksandrov[b]

[a] *Research Institute of Chemistry, Lobachevskii Nizhny Novgorod National Research University, pr. Gagarina 23, build. 5, Nizhny Novgorod, 603950 Russia*
e-mail: didenkul@mail.ru

[b] *Lobachevskii Nizhny Novgorod National Research University*

Received November 11, 2010

Abstract—Kinetic and activation parameters of carbon monoxide oxidation on catalysts prepared by pyrolysis of the transition metals β-diketonates on synthetic ceramic foam matrices of different nature were measured in the absence of oxygen in the reaction mixture. Based on the kinetic data and infrared spectroscopy, the contributions of *conjoint* and *split* reaction mechanisms of CO oxidation as a function of temperature and nature of the carrier were estimated.

DOI: 10.1134/S1070363212020120

Analysis of published data on the mechanism of catalytic oxidation of CO shows that for the description of this process two different mechanisms are suggested [1]: the *conjoint* (Langmuir–Hinshelwood), occurring at low temperatures, and the *split* (Mars–Van Krevelen or Rideal–Eley), which is realized at higher temperatures. In the first case, oxygen and carbon monoxide are adsorbed on active centers of the catalyst, and then in the adsorbed state react with each other. For the second mechanism the separate interaction of CO and O_2 with the catalyst surface is characteristic: Initially, the surface of the catalyst is reduced with carbon monoxide, and then it is oxidized by the gas phase oxygen to surface oxides. However, recently data appeared on the occurrence of CO oxidation at low temperatures by the *split* mechanism [2–5].

In this paper the CO to CO_2 oxidation was performed in the absence of oxygen in the gas mixture in order to establish the mechanism of the oxidation on the catalysts prepared by the gas-phase thermal decomposition of transition metals β-diketonates in a vacuum on a synthetic ceramic foam.

The catalyst carriers were prepared using a modified "HIPEK" ceramic foam samples [6], one of them, prepared from environmentally pure product, the natural clay of montmorillonite type, heat resistant to 760°C, which was shown earlier [7] to be inert, (carrier **I**), another sample is active, obtained from the galvanic production wastes (carrier **II**). On these matrices, using gas-phase thermal decomposition under vacuum (CVD), solid-phase products of thermal decomposition of transition metal acetylacetonates (M = Cu, Co, Mn, Zr, Fe, Cr), and nickel hexafluoroacetylacetonate, Ni(*hfacac*)$_2$ were applied. The composition of the catalysts, the conditions of their preparation and processing are given in Table 1.

Thermal decomposition of a β-diketonate complex is known [8] to afford a metal–carbon composite coatings containing metal, its oxide and carbide, as well as free carbon. All the obtained coatings were heated for 1 h at 600ºC to convert the metals in oxide form and to remove the unbound carbon.

The investigation of the catalytic activity of catalysts was carried out in a pulse microcatalytic system.

Table 2 lists the activation parameters of CO oxidation in the absence of oxygen. Under these conditions only *split* mechanism of the oxidation of CO by oxygen lattice can be realized. The catalyst activity was derived from the temperature corresponding to 10% transformation of the original

Table 1. Catalysts of oxidation of CO to CO_2 prepared by thermal gas phase decomposition (CVD): composition and conditions of preparation and processing

Catalyst composition	Designation	Source of metal	Conditions of the metal deposition
Carrier **I** + 3% Co	Co/**I**	Co(*acac*)$_2$	320°C, 2 h
Carrier **I** + 3% Mn	Mn/**I**	Mn(*acac*)$_2$	400°C, 1 h
Carrier **I** + 3% Zr	Zr/**I**	Zr(*acac*)$_4$	350°C, 2 h
Carrier **I** + 3% Fe	Fe/**I**	Fe(*acac*)$_3$	400°C, 1 h
Carrier **I** + 3% Cr	Cr/**I**	Cr(*acac*)$_3$	400°C, 1 h
Carrier **I** + 3% Ni	Ni/**I**	Ni(*hfacac*)$_2$	350°C, 1 h
Carrier **I** + 3% Cu	Cu/**I**	Cu(*acac*)$_2$	350°C, 1 h
Carrier **I** + 3% Mn + 3% Ni	Mn–Ni/**I**	Mn(*acac*)$_2$ Ni(*hfacac*)$_2$	400°C, 1 h
Carrier **I** + 3% Mn + 3% Cu	Mn–Cu/**I**	Mn(*acac*)$_2$ Cu(*acac*)$_2$	400°C, 1 h
Carrier **I** + 3% Cu + 3% Ni	Cu–Ni/**I**	Cu(*acac*)$_2$ Ni(*hfacac*)$_2$	350°C, 1 h
Carrier **I** + 3% Co + 3% Cu	Co–Cu/**I**	Co(*acac*)$_2$ Cu(*acac*)$_2$	300°C, 2 h
Carrier **II** + 3% Co	Co/**II**	Co(*acac*)$_2$	320°C, 2 h
Carrier **II** + 3% Mn	Mn/**II**	Mn(*acac*)$_2$	400°C, 1 h
Carrier **II** + 3% Zr	Zr/**II**	Zr(*acac*)$_4$	350°C, 2 h
Carrier **II** + 3% Fe	Fe/**II**	Fe(*acac*)$_3$	400°C, 1 h
Carrier **II** + 3% Cr	Cr/**II**	Cr(*acac*)$_3$	430°C, 1 h
Carrier **II** + 3% Ni	Ni/**II**	Ni(*hfacac*)$_2$	350°C, 1 h
Carrier **II** + 3% Mn + 3%Ni	Mn–Ni/**II**	Mn(*acac*)$_2$ Ni(*hfacac*)$_2$	400°C, 1 h
Carrier **II** + 3% Mn + 3%Cu	Mn–Cu/**II**	Mn(*acac*)$_2$ Cu(*acac*)$_2$	400°C, 1 h
Carrier **II** + 3% Cu + 3% Ni	Cu–Ni/**II**	Cu(*acac*)$_2$ Ni(*hfacac*)$_2$	350°C, 1 h
Carrier **II** + 3% Co + 3% Ni	Co–Ni/**II**	Co(*acac*)$_2$ Ni(*hfacac*)$_2$	300°C, 1 h

components. On the carrier **I** the catalysts are arranged by activity as follows: Cu–Ni/**I** > Cu/**I** > Mn–Cu/**I** > Cr/**I** > Mn/**I** = Ni/**I** > Zr/**I** > Fe/**I** > Co/**I** > Mn–Ni/**I**.

Activity of the catalysts on carrier **I** in the absence of oxygen decreases, the curves of CO conversion to CO_2 are shifted to higher temperatures by 50–150°C compared with the conversion in the presence of oxygen [9]. Under these conditions the Cu-containing catalysts have the highest activity: Cu–Ni/**I**, Cu/**I** and Mn–Cu/**I**, and the Mn–Ni/**I** catalyst is the least active (Fig. 1). It is noted that the whole series of catalysts on the carrier **I** shows the same activity sequence both in the presence and in the absence of oxygen in the reaction mixture.

On carrier **II** (Fig. 2) in the absence of oxygen in the mixture the CO conversion to CO_2 on all catalysts

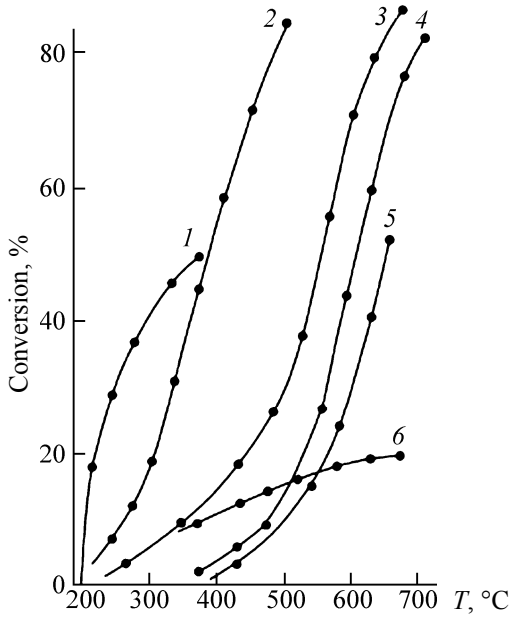

Fig. 1. Comparison of catalytic activity of catalysts on the carrier **I** (F = 0.5 cm^3 s^{-1}, fraction 0.3–0.5 mm) in the absence of oxygen in the reaction mixture. Catalysts: (*1*) Cu–Ni/**I**, (*2*) Cu/**I**, (*3*) Cr/**I**, (*4*) Zr/**I**, (*5*) Fe/**I**, (*6*) Ni/**I**.

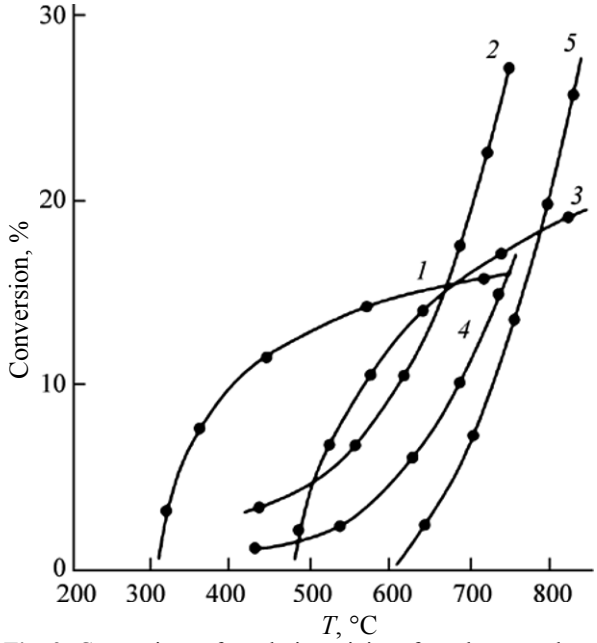

Fig. 2. Comparison of catalytic activity of catalysts on the carrier **II** (F = 0.5 cm^3 s^{-1}, fraction 0.3–0.5 mm) in the absence of oxygen in the reaction mixture. Catalysts: (*1*) Ni/**II**, (*2*) Cr/**II**, (*3*) Zr/**II**, (*4*) Co–Ni/**II**, (*5*) Fe/**II**.

Table 2. Activation parameters of the reaction of catalytic oxidation of CO to CO_2 in the absence of oxygen on the catalysts prepared by thermal gas phase decomposition

Catalyst	Temperature range, °C	T, °C for α = 10%	log k_0	$E^{apparent}$, kJ mol^{-1}
Co/**I**	350–725	600	3.45±0.52	70.4±2.1
Mn/**I**	365–675	450	3.73±0.25	50.5±3.4
Zr/**I**	460–660	520	4.51±0.15	80.4±2.3
Fe/**I**	415–670	540	4.42±0.73	83.9±2.5
Cr/**I**	275–675	325	2.28±0.32	37.8±4.4
Ni/**I**	270–600	450	0.86±0.37	24.3±5.6
Cu/**I**	225–500	275	3.16±0.10	41.9±1.1
Mn–Ni/**I**	435–763	625	3.81±0.86	83.9±3.6
Mn–Cu/**I**	192–540	300	3.81±0.24	46.1±1.4
Cu–Ni/**I**	200–350	210	2.13±0.35	26.1±3.3
Co/**II**	275–70	480	0.85±0.13	27.2±1.9
Mn/**II**	500–800	680	2.94±0.09	69.0±1.6
Zr/**II**	382–765	610	1.92±0.50	51.9±4.4
Fe/**II**	684–800	760	4.74±0.37	111.8±7.3
Cr/**II**	400–750	615	0.13±0.1	37.7±1.5
Ni/**II**	300–712	450	0.67±0.10	24.9±5.6
Mn–Ni/**II**	375–750	580	3.44±0.42	70.4±3.6
Mn–Cu/**II**	400–750	550	4.0±0.74	76.6±3.3
Cu–Ni/**II**	425–825	680	2.41±0.06	63.5±1.0
Co–Ni/**II**	290–740	600	0.83±0.11	27.3±1.82

decreases. Conversion curves are shifted to higher temperatures compared with conversion in the presence of oxygen even by 200–400°C, and at 700°C the conversion does not exceed 15%. On carrier **II** the following sequence of catalysts by their activity was obtained: Ni/**II** > Co/**II** > Mn–Cu/**II** > Mn–Ni/**II** > Co–Ni/**II** > Zr/**II** ≥ Cr/**II** > Cu–Ni/**II** ≥ Mn/**II** > Fe/**II**.

Thus, the Ni-containing catalyst has the greatest activity, and the lowest activity corresponds to the Fe-containing catalyst. The activity of the catalysts on carrier **II** in the absence of oxygen is much lower compared to the catalysts obtained on carrier **I** (Figs. 1, 2).

It is known [10] that the oxidation of CO on the catalyst surface in the absence of oxygen occurs due to the oxygen of the carrier crystal lattice. Therefore, the activity of catalysts in the absence of oxygen is determined to a greater extent by the nature of the carriers themselves. The composition of the carrier **I** contains oxides, which may release oxygen for the CO oxidation in the absence of oxygen in the gas mixture, while the carrier **II** consists mainly of metal salts (chlorides, sulfates and phosphates).

To confirm this hypothesis and to study the oxidation mechanism in more detail we measured IR spectra of the most active catalysts before and after CO

Table 3. Dependence of CO to CO_2 conversion on the temperature in the presence (α_1) and absence (α_2) of oxygen on the catalysts obtained on carriers **I** and **II**

Catalyst on carrier **I**	*T*, °C	α_1, %	α_2, %	$(\alpha_2/\alpha_1)\times100$, %	Catalyst on carrier **II**	*T*, °C	α_1, %	α_2, %	$(\alpha_2/\alpha_1)\times100$, %
Co/**I**	400	51	1	2	Co/**II**	300	20	2	10
	500	16	4	25		400	82	5	6.1
	650	40	25	62.5					
Cr/**I**	300	33	10	30.3	Cr/**II**	400	51	2.2	4.3
	400	62	20	32.3		425	81.3	2.5	3.1
	550	100	50	50					
Ni/**I**	300	66	2.5	3.8	Ni/**II**	328	90.5	4	4.4
	340	76.6	8	10.4		340	98	5	5.1
	350	80	8.5	10.6					
Cu/**I**	250	25	7.5	30	Co-Ni/**II**	235	40.7	0	0
	325	75	25	33.3		275	75.8	0	0
	400	90	55	61.1		330	95.2	0	0
Fe/**I**	415	8	1.9	23.7	Fe/**II**	315	21.8	0	0
	620	63.2	28.4	45		340	38.3	0	0
	670	100	50.5	50.5		368	75.8	0	0

oxidation [7]. Applying active metals on supports **I** and **II** did not alter the shape of the IR spectra of the carriers themselves, which is caused by low metal content (less than 5%). Therefore, the infrared spectra of the catalysts Co–Ni/**II** and Co–Cu/**I** before the oxidation are identical to the IR spectra of the carriers themselves. We registered the IR spectra of these catalysts before and after CO oxidation.

The IR spectra of the catalyst Co–Ni/**II**, obtained on the carrier **II**, before and after the oxidation reaction in the absence of oxygen in the reaction mixture remained unaltered. The IR spectra of the catalyst Co–Cu/**I** obtained on a carrier **I,** before and after oxidation in the presence of oxygen in the reaction mixture were significantly different [7]. In this case, the area of the transmission band corresponding to vibrations of the Si–O group increased, suggesting that carbon monoxide is oxidized by the oxygen from the carrier **I**. Thus, it was confirmed that the oxidation of CO on the catalysts obtained on the carrier **I** occurs with the participation of the oxygen from the matrix.

Table 3 shows the ratio of conversions (α_2/α_1) at different temperatures, where α_1 is the conversion of CO to CO_2 in the presence of oxygen when the O_2 and CO are adsorbed on active centers of the catalyst and react with each other, α_2 is the conversion in the absence of oxygen, when oxidation is due to the crystal lattice.

The oxidation on catalysts obtained on carrier **I** in the presence of oxygen proceeds through two mechanisms: First it is *conjoint* (Langmuir–Hinshelwood) mechanism. It occurs at low temperatures, and then, upon reaching a certain temperature, the *split* (Mars–van Krevelen) mechanism of the oxidation starts to operate. Moreover, the temperature of the transition to *split* mechanism is quite definite for each catalyst, and it coincides with the temperature where the catalyst begins to work in the absence of oxygen. On the catalysts based on carrier **II** the oxidation of carbon monoxide proceeds mainly according to the *conjoint* mechanism, the contribution of the *split* mechanism for many of them is so small that it can be ignored. Table 3 shows the contribution of the *split* mechanism in the process of oxidation on the catalysts at various temperatures. With the catalyst on carrier **I** the contribution of the *split* mechanism increases with temperature, while with the catalyst on **II** the contribution of the *split* mechanism is small and decreases with temperature.

The studied catalysts show a compensation effect, which is described quantitatively by the Kremer–Constable relation [11]:

$$\ln k = bE_a + c,$$

where k is the pre-exponential factor; b and c are constant, E_a is activation energy. In the presence of the compensation effect, a decrease in the activation energy of the reaction on different modified catalysts is accompanied by a decrease in the frequency factor. Figure 3 shows the compensation effects of CO

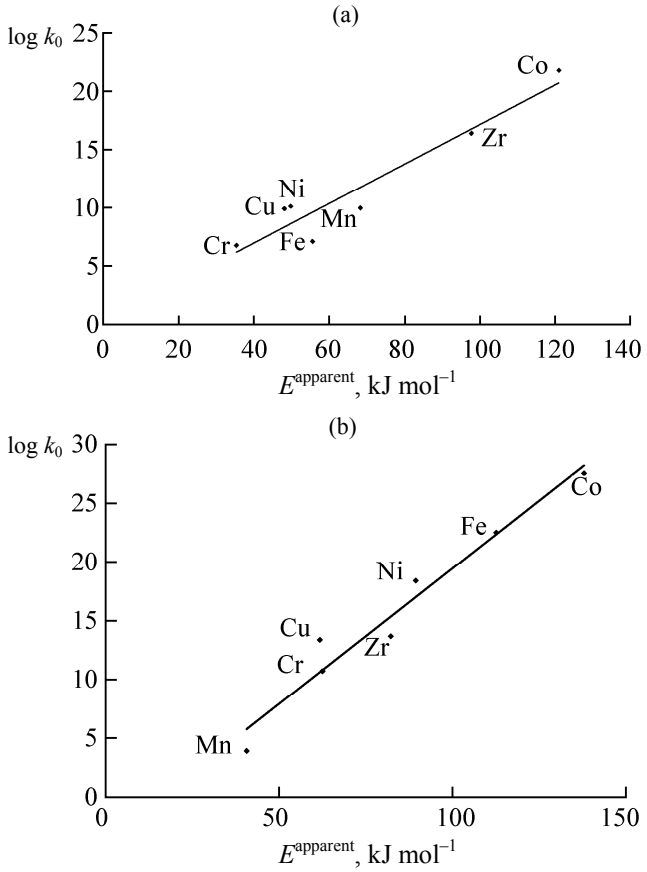

Fig. 3. Compensation effect in the reaction of CO oxidation in the presence of atmospheric oxygen on monometallic catalysts: (a) based on carrier **I**. The correlation coefficient ρ = 0.91, θ = 435°C, (b) based on carrier **II**. The correlation coefficient ρ = 0.96, θ = 249°C.

oxidation in the presence of oxygen on the catalysts based on carriers **I** and **II**. The presence of the compensation effect suggests that the studied CO oxidation on different catalysts occurs by the general mechanism. The slope of the lines in Fig. 3 is equal to 1/(Rθ), where R is the universal gas constant, and we can determine the isokinetic temperature θ, at which the rate of the reactions studied on all the catalysts of this group is the same.

Low correlation coefficient in Fig. 3a, for the monometallic catalysts based on the carrier **I** is due to the fact that the reaction mechanism of CO oxidation on these catalysts is complex. At low temperatures acts the *conjoint* mechanism, but with increasing temperature the *split* mechanism is added, when the bulk phase of the carrier begins to participate in the catalytic act of CO oxidation. Both mechanisms work simultaneously, but the contribution of the *split* one increases with temperature, and temperature at which the *split* mechanism begins to work is different for different catalysts.

A higher correlation coefficient of the compensation effect for the monometallic catalysts based on carrier **II** (Fig. 3b) indicates that the mechanism of CO oxidation is common for the whole group of catalysts, regardless of the nature of transition metal. On these catalysts the *conjoint* or adsorption mechanism of CO oxidation dominates.

Thus, it was established experimentally that the activity of these catalysts of CO oxidation in the absence of oxygen in the gas mixture depends largely on the presence of oxides in the carrier.

EXPERIMENTAL

Preparation of carriers for catalysts based on the HIPEK ceramic was carried out in accordance with the TU 5759-010-10657190-97 [6], by introducing a system of various fillers and additives. To prepare the catalyst samples ceramics were taken annealed for 1 h at 500ºC (fraction 0.3–0.5 mm).

The carrier–promoting additive ratios are given in Table 1. A weighed sample of carrier with an estimated amount of the β-diketonate additive was placed in a 60 ml glass ampule. The ampule was evacuated and placed in a furnace heated to a desired temperature. The optimum conditions for thermal decomposition of β-diketonates [12] were chosen. The obtained catalysts were annealed in air for 1 h at 600ºC.

Kinetics of heterogeneous catalytic oxidation of CO to CO_2 was studied by the pulse version of the gas chromatography method. The conversion was calculated from the CO_2 peaks by the method of calibration.

The IR spectra of samples of carriers **I** and **II** ground with KBr and pressed and of similarly prepared samples of catalysts based on these carriers were recorded on a Shimadzu infrared Fourier spectrometer IR Prestige 21.

REFERENCES

1. Dorfman, Ya.A., *Katalizatory i mekhanizmy gidrirovaniya i okisleniya* (Catalysts and Mechanismes of Hydrogenation and Oxidation), Alma-Ata: Nauka, 1984.
2. Liu, W. and Flytzanistephanopoulos, M., *J. Catal*., 1995, vol. 153, no. 2, p. 317.
3. Sedmak, G., Hocevar, S., and Levec, J., *J. Catal*., 2003, vol. 213, no. 2, p. 135.

4. Il'ichev, A.N., Firsova, A.A., and Korchak, V.N., *Kinetika i Kataliz*, 2006, vol. 47, no. 4, p. 602.
5. Snytnikov, P.V., Stadnichenko, A.I., Semin, G.L., Belyaev, V.D., Boronin, L.I., and Sobyanin, V.A., *Kinetika i Kataliz*, 2007, vol. 48, no. 3, p. 472.
6. Aleksandrov, Yu.A., Shekunova, V.M., Tsyganova, E.I., and Didenkulova, I.I., RF Patent no. 2345973, 2008; *Byul. Izobret*., 2009, no. 4.
7. Didenkulova, I.I., Tsyganova, E.I., Shekunova, V.M., Kirillov, A.I., Pishchurova, I.A., and Aleksandrov, Yu.A., *Vestnik Nizhegorod. Gos. Univ., Ser. Khim*., 2008, no. 3, p. 79.
8. Suvorova, O.N., Varyukhin, V.A., and Kutyreva, V.V., *Primenenie metalloorganicheskikh soedinenii dlya polucheniya neorganicheskikh pokrytii i materialov* (Use of Organimetallic Compounds for Obtaining Coverings and Materials), Razuvaev, G.A., Ed., Moscow: Nauka, 1986, p. 68.
9. Tsyganova, E.I., Didenkulova, I.I., Shekunova, V.M., and Aleksandrov, Yu.A., *Vestnik Nizhegorod. Gos. Univ., Ser. Khim*., 2007, no. 2, p. 95.
10. Guglielminotti, E., Boccuzzi, F., Manzoli, M., Pinna, F., and Scarpa, M., *J. Catal*., 2000, vol. 192, no. 1, p. 149.
11. Bremer, G. and Vendlandt, K.–P., *Vvedenie v geterogennyi kataliz* (Introduction to Heterogenous Catalysis), Moscow: Mir, 1981, p. 81.
12. Gribov, B.G., Domrachev, G.A., Zhuk, B.V., Kaverin, B.S., Kozyrkin, B.I., Mel'nikov, V.V., and Suvorova, O.N., *Osazhdenie plenok i pokrytii razlozheniem metalloorganicheskikh soedinenii* (Filming and Covering by Decomposition of Organometallic Compounds), Moscow: Nauka, 1981.